International Journal of Mass Spectrometry 470 (2021) 116703

Contents lists available at ScienceDirect

International Journal of Mass Spectrometry

journal homepage: www.elsevier.com/locate/ijms

Varying the aspect ratio of toroidal ion traps: Implications for design, performance, and miniaturization

Praneeth M. Hettikankanange, Daniel E. Austin*

Department of Chemistry and Biochemistry, Brigham Young University, Provo, UT, USA

ARTICLE INFO

Article history:
Received 1 May 2021
Received in revised form
23 August 2021
Accepted 6 September 2021
Available online 8 September 2021

Keywords:
Toroidal ion trap
Aspect ratio
Saddle point
Geometric center
Higher-order multipoles
Secular frequency

ABSTRACT

A large aspect ratio (AR) leads to higher ion capacity in miniaturized ion trap mass spectrometers. The AR of an ion trap represents the ratio between an extended trapping dimension and the characteristic trapping dimension. In contrast to linear and rectilinear traps, changing the AR of a toroidal ion trap (TorIT) results in changes to the degree of curvature and shape of the trapping potential, and hence, on performance as a mass analyzer. SIMION simulations show that higher-order terms in the trapping potential vary strongly for small and moderate AR values (below ~10), with the effects asymptotically flattening for larger AR values. Because of the asymmetry in electrode geometry, the trapping center does not coincide with the geometric center of the trap, and this displacement also varies with AR. For instance, in the asymmetric TorIT, the saddle point in the trapping potential and the geometric trap center differ from +0.6 to −0.4 mm depending on AR. Ion secular frequencies also change with the AR. Whereas ions in the simplified TorIT have stable trajectories for any value of AR, ions in the asymmetric TorIT become unstable at large AR values. Variations in high-order terms, the trapping center, and secular frequencies with AR are a unique feature of toroidal traps, and require significant changes in trap design and operation as the AR is changed.

1. Introduction

Portable mass spectrometry seeks to make real-time, in situ chemical measurements of complex or rapidly varying systems in their original environment, promising significant opportunities and advantages in many fields of science. Many advances in the development of portable mass spectrometers have been driven by the challenges of maintaining analytical performance while making instruments smaller, lighter, and more rugged, while others are based on reducing the cost and operational complexity of such systems to promote wider use [1–7]. Ion traps are one of the most common types of mass analyzers used in miniaturization efforts due to their inherently small size, tolerance to higher pressures, and ability to perform tandem mass analysis on complex samples. However, ion traps are by no means simple devices, and miniaturization efforts have led to many changes and improvements in trap design and operation. For example, simplifying the electrode geometry is of particular utility for miniaturizing ion trap mass analyzers [5,6,8] because the ideal hyperbolic electrode shapes are difficult to produce accurately at small scales. Cylindrical ion traps (CITs) and the rectilinear ion trap (RIT) address this particular issue, as the planar and cylindrical electrode shapes can be made with better precision. Electrode positioning and alignment, and even surface smoothness can all affect the ion trap performance and become more significant at smaller scales [9,10].

As an example of another issue, reducing the physical size of the ion trap allows for lower RF voltages and higher-pressure operation, but comes at the cost of reduced trapping capacity and reduced sensitivity. Parallel arrays of cylindrical ion traps increase total trapping capacity by having multiple traps, although any dimensional variation between traps results in reduced mass resolution [2]. The issue of reduced trapping capacity is also addressed in ion traps with an extended trapping dimension, such as toroidal [1,4,11,12], linear [13], and rectilinear ion traps [8]. Trapped ions are able to spread out along this extended trapping dimension, reducing space-charge effects and allowing more ions to be trapped. At the same time, the trapping voltage and frequency—and typically the tolerable operating pressure—are governed by the characteristic trapping dimension, which is typically the dimension of ion ejection. The characteristic trapping dimension is typically

* Corresponding author.
E-mail address: austin@chem.byu.edu (D.E. Austin).

https://doi.org/10.1016/j.ijms.2021.116703
1387-3806/

perpendicular to the extended trapping dimension. For a miniaturized device, this characteristic trapping dimension is reduced, realizing the benefits of lower electrical power and higher operating pressure, while the trapping capacity is retained through the extended trapping dimension.

The aspect ratio (AR) of such an ion trap is defined as the ratio between the extended trapping dimension, R_0, and the characteristic trapping dimension, r_0, such that AR = R_0/r_0. Although a high AR would seem to offer the best of both worlds—the benefits of miniaturization without the loss of sensitivity—several practical issues must also be addressed. For example, the tolerable misalignment of electrodes scales with the characteristic trapping dimension, becoming more difficult for high AR traps [9–12,14]. Collecting ions ejected from a long ejection slit onto a small detector may also present ion focusing challenges. In the case of linear and rectilinear traps, axial trapping using DC potentials on endcaps concentrates ions at the trap center, but this increases space-charge effects and reduces trapping capacity. Toroidal ion traps are able to focus ions radially onto a small detector, but changing the AR also changes the shape of the trapping potential itself.

Toroidal ion traps (TorIT) are based on a quadrupole-like cross-section, but rotated using an axis of rotation located outside of the quadrupole cross-section [12] (Fig. 1). Thus, the AR of a TorIT can be defined as the ratio between the trap's annular radius (inscribed toroidal radius, R_0) to the characteristic trapping radius (r_0). The extended trapping dimension has length $2\pi R_0$, and ions are able to spread out along the entire ring; however, we will use R_0 in the definition of AR for simplicity. As with the other types of ion traps, a version of the toroidal ion trap has been developed using simplified geometry (the Simplified Toroidal Ion Trap, or STorIT), with all electrodes either as planar or cylindrical surfaces [6]. In the asymmetric TorIT, two different asymptote angles were assigned for the electrode geometry: one for surfaces located closer to the rotational axis than R_0 and the second for surfaces beyond R_0 [12].

In contrast to all other types of ion traps, changing the AR of a toroidal ion trap results in changes to the degree of curvature and the shape of the trapping potential and, ultimately, the performance as a mass analyzer. Understanding these changes, including the higher-order terms in the trapping potential, are important to understanding the relationship between performance and AR, and are key to developing an instrument that benefits from lower power and higher-pressure operation while maximizing sensitivity. Previous studies have shown that the curvature of the toroidal trapping region results in several effects. For example, Lammert showed that the symmetric TorIT suffers from poor mass resolution because of the additional fields contributed by the curvature of the device [12]. Higgs and Austin showed using ion trajectory simulations that the curvature of the trap causes ions to experience a centripetal-like effect which can shift the ion motion outward from the saddle point in the trapping potential [15]. The effects of curvature will be directly impacted by the choice of AR, and will impact performance as a miniaturized device. Finally, as the AR of the toroidal trap becomes very large, as may be done to increase trapping capacity, curvature effects disappear and the fields within the device look more and more like those of a LIT.

In other types of ion traps, an analysis of the higher-order terms in the trapping potential are helpful to understand and optimize performance [8,10,16]. The cumulative effect of these terms is that frequency of an ion's secular motion becomes dependent on amplitude. The shift of secular frequency affects ion ejection, mass resolution, and mass accuracy for resonantly ejected ions. Thus, higher-order terms in the trapping potential can be leveraged for improved performance.

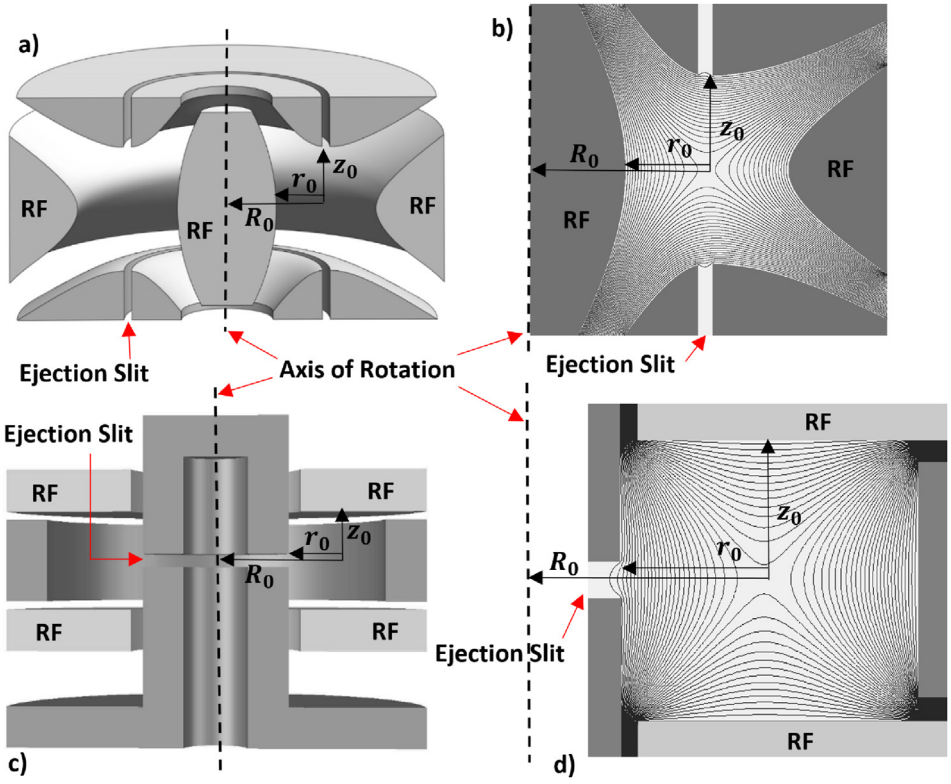

Fig. 1. Cross-section views of asymmetric TorIT (a–b) and simplified TorIT (c–d). RF electrodes are indicated; the remaining electrodes are normally held at ground or with small AC waveforms for ion excitation or ejection. The dimensions for the asymmetric TorIT and simplified TorIT were taken from Lammert et al. [12] and Taylor and Austin [6], respectively. The aspect ratio (AR) of any TorIT is defined as the ratio between the annular radius (inscribed toroidal radius) (R_0) to the trap radius r_0. Images (b) and (d) show the isopotential contours of the corresponding trapping regions.

In this study, we analyze the response of key TorIT parameters to the change of AR. We also compare the response of these parameters with two different TorIT designs including the simplified TorIT with radial ejection and the asymmetric TorIT with axial ejection. We observe changes in the higher-order terms, shift of the saddle point compared to the geometric trapping center, and dependency of the secular frequency on AR. Understanding such relationships could help to optimize the performance of the trap in the design stage and provide a foundation to develop a mathematical relationship between the stability parameters and AR.

2. Methods

SIMION 8.0 (Scientific Instrument Services, Ringoes, NJ) was used to simulate the behavior and performance of the asymmetric and simplified TorIT with different aspect ratios. The electrode cross-sections shown in Fig. 1(b) and (d) were kept constant; that is, no attempt was made to re-optimize the electrode shape as the AR was changed. This allowed observation of the ways the trapping field and resulting ion behavior changed with AR as the only variable. The simplified TorIT dimensions used for the simulations in this project were taken from Taylor and Austin [6] while the asymmetric TorIT dimensions were taken from Lammert et al. [12]. The r_0 values and aspect ratios of these traps as originally presented were $r_0 = 10$ mm, AR = 2.54 (asymmetric) and $r_0 = 5.8$ mm, AR = 6.1 (simplified). Using the cross-sections of both designs we also investigated the effect of ARs starting from 1.86 and increasing until 47.75, by which point the AR-dependence of all parameters became negligible. Consistent with the above references, we used radial ejection in the simplified TorIT and axial ejection in the asymmetric trap. Due to reflection symmetry about the radial plane, the saddle point of the trapping potential in the simplified TorIT always aligns exactly with the ejection slit. However, in the asymmetric TorIT with axial ejection, the position of the saddle point changes with the AR. For these simulations, we positioned the exit slits directly above and below the saddle point (more correctly, a saddle ring) in the potential. The location of the slits was adjusted for each AR studied to keep them aligned exactly with the trapping center.

The scale used both for the simplified and asymmetric TorIT simulations was 0.0125 mm per grid unit. The symmetry of the electrodes in SIMION was set to cylindrical. For evaluating the shape of the trapping potential distribution, the RF electrodes were set to 500 V, with 0 V applied to the remaining electrodes. The potential was recorded at each point along the ejection direction of the trap, following a linear trajectory from the center of the slit to the other end on the electrode through the geometric trapping center. The potential was recorded at each grid unit.

The resulting data was then imported into MATLAB R2017a (The Math Works, Natick, MD) for analysis. The positions in the ejection direction were normalized relative to the trap radius. The reason for the use of normalized positions along the ejection direction is to avoid the higher-order terms having different units. The potential profile along the ejection direction was analyzed by fitting the normalized points to a polynomial function. The built-in ***polyfit*** function in MATLAB was used to construct the polynomial function. Rather than using all data points contained within the trapping region, only the 400 points centered on the saddle point (out of 1000 points total) were used for the higher-order multipole calculation. The reason for using a subset of data points was to avoid the fringe effect near the electrodes. Many other efforts to evaluate higher-order multipoles in ion traps have fitted the potentials to polynomial functions of order 20–25 [6,9,15,17–19]. To determine the optimal order of the polynomial function for the present work, we determined the variance of the polynomial function for polynomial fits from the 6th to the 25th order. We also examined the effects of using data points spanning different distances on both sides of the saddle point. The 8th-order polynomial fit with 400 data points (representing 40% of the entire data set) gave the lowest variance compared to other polynomial function orders and different fractions of the total data set. The coefficients obtained from the polynomial function were then used to calculate the magnitude of the hexapole (A_3) octopole (A_4), decapole (A_5), and dodecapole (A_6) components. Higher-order field contributions (A_n/A_2%) were then normalized by taking the percentage relative to the quadrupole (A_2) term. These higher-order terms are only applicable near the trapping center: the conventional Cartesian multipoles used to describe other types of ion traps are not strictly valid, mathematically, for toroidal traps. At the axis of rotation, a non-zero electric field cannot be continuous and differentiable, violating the Laplace equation. There is also no *a priori* reason for higher-order terms to all be centered at the same radial distance (in this case, at R_0). Nonetheless, expressing the conventional multipoles in the vicinity of the trapping center is still useful to help qualitatively understand ion behavior in toroidal traps.

To investigate the secular frequency of ions with no collision gas, for each trap geometry an ion with $m/z = 100$ Th was simulated with the trap operating at RF = 500 $V_{0\text{-}p}$ and a frequency of 1 MHz. This m/z value as chosen as a representative ion mass for small molecule analysis. While the specific values of mass resolution and ion ejection efficiency will likely differ for ions of different m/z, the trends with AR should be similar. The initial velocity components of each ion along the radial, axial and tangential directions were set to 0.1 mm/μs. In each simulation the ion was introduced at a point 0.5 mm towards the outer electrode from the saddle point. This ion velocity and position offset corresponds approximately to a thermalized ion (hypothetical in this collisionless case) and were selected because they result in secular motion that is small relative to the electrodes. This results in a signal unperturbed by collisions yet long enough for adequate Fast Fourier Transform function (FFT) analysis. The position (x,y,z) of the ion was recorded every 0.01 μs. To take advantage of the improved accuracy of the (FFT) from using 2^n data points, 8192 data points were recorded for each simulation. The coordinates of the position of the ion with respect to time were converted to axial, angular, and radial positions, and the average radial position was also calculated. The frequency spectrum of the ion was then evaluated with MATLAB's ***FFT*** to identify the frequencies of the ion motion.

Ion ejection in the simplified TorIT was investigated using mass-selective ejection under the same conditions used above, with an auxiliary AC voltage applied on the outer electrode ($V_{0\text{-}p} = 2$ V) to excite the ion via dipolar resonant ejection. The frequency for the AC voltage was set to a value that is a few percent lower than the exact secular frequency of the ion [20]. This percentage was the minimum amount required to eject the ion from the trap, and was manually determined by running multiple simulation runs. Collision effects were incorporated into the SIMION user program using a hard-sphere model. The pressure and temperature of the system were set to 1.5 mTorr and 273 K. The number of ions ejected from the trap was calculated by a user program segment added to the main LUA program.

3. Results and discussion

The polynomial equations from mapping the potentials in both designs were used to determine the higher-order field contribution of A_3, A_4, A_5, and A_6 normalized to the A_2 term. Fig. 2 (a and b) shows the dependency of higher-order terms with AR in the simplified TorIT with radial ejection and the asymmetric TorIT with axial ejection. The simplified TorIT with radial ejection has

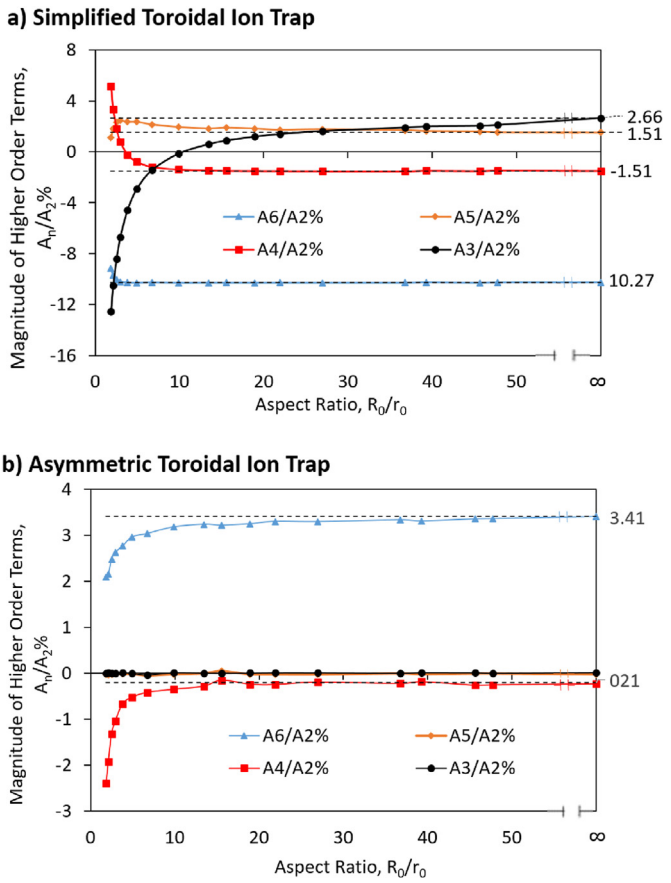

Fig. 2. Effect of aspect ratio on the normalized hexapole [$(A_3/A_2) \times 100\%$], octopole [$(A_4/A_2) \times 100\%$], decapole [$(A_5/A_2) \times 100\%$], and dodecapole [$(A_6/A_2) \times 100\%$] in the simplified TorIT in the radial direction (a) and asymmetric TorIT in the axial direction (b). The trapping radius, r_0, was held constant at 10 mm and 5.8 mm for asymmetric TorIT and simplified TorIT respectively. The last points represent the corresponding higher-order terms of a linear-type ion trap (LIT) with the same electrode cross-section as the corresponding toroidal trap.

contributions from odd-order terms along the radial direction, as shown in Fig. 2(a). For ion traps with reflection symmetry about the central plane, the dipole term (A_1), and all higher odd-order terms vanish due to symmetry [15]. This is the case for axial ejection in the asymmetric ion trap (Fig. 2(b)) where all the odd-order terms including hexapole and decapole terms are approximately zero regardless of the AR. In this case, there are still curvature effects [15], but they are not represented in the odd-order terms of the trapping potential because the multipole expansion is oriented in the axial rather than radial directions. If higher-order terms are centered, or are symmetric around, a point other than R_0, this will be reflected as additional deviations from the multipole analysis shown in Fig. 2.

Non-linearity of the electric field in an ion trap is typically caused by ejection holes or slits, by electrode truncation [21], by irregularities on the electrode surface [10], by misalignment of the electrodes [9–12,14], or by non-ideal electrode shape or spacing. For toroidal traps, the curvature of the toroidal trapping region also affects field non-linearity [12,15]. At lower ARs, the degree of the curvature of the inner and outer electrodes are very significant. The curvature effects can strongly influence trapped ions. Not surprisingly, the curvature effect becomes less significant at higher ARs. Fig. 2 shows that the higher order terms are very sensitive to changes in AR for small values of AR, becoming less sensitive at larger values of AR. Nearly all higher-order terms drop off smoothly as AR increases. The decapole (A_5/A_2) in the Simplified toroidal trap shows an unusual dip at the lowest AR studied—this feature is not present in the other trap, and the origin of the feature is unclear. This figure also shows that the magnitudes of the higher-order terms become large when the AR is very different from that originally used for designing these traps. In other words, the simplified TorIT was originally designed with an AR of 6.1, but as the AR drops below this and approaches lower values, the hexapole and octopole terms deviate dramatically. The deviations of these terms in the asymmetric trap are not as great, likely because the trap was originally designed for an AR of only 2.54.

Fig. 2 shows a large hexapole component in the ejection direction of the simplified toroidal ion trap for small AR values. This large hexapole component is partly responsible for the observed ability to ejection ions in only one direction [6]. Unidirectional ejection increases the number of ions detected compared with ion traps in which ions are ejected equally in two directions. In contrast, due to symmetry the hexapole (A_3/A_2) and decapole (A_5/A_2) are essentially zero in the ejection direction of the asymmetric toroidal ion trap (in this case the axial direction).

In addition to changing the higher-order terms of the trapping potential, changing the AR can also shift the location of the saddle point of a TorIT. The saddle point is the point where the potential reaches its maximum or minimum in the trapping region. Due to symmetry, in quadrupole and linear traps the saddle point and geometric trap center coincide. However, as noted by Kotana and Mohanty [22] and also seen in our SIMION simulations, in toroidal traps the geometric trap center and saddle point generally do not coincide. This has particular consequence in TorITs with ion ejection along the axial direction, where alignment between trapping center and ejection slits impacts the ion ejection process. With radial ejection, the saddle point remains aligned along the ejection slits, although its radial position still changes with AR.

Fig. 3 shows that the separation between the saddle point of the trapping potential and the geometric trap center varies as a function of AR in both asymmetric and simplified TorITs. The location of the saddle point follows from Coulomb's Law and is dependent on the electrode geometry and placement. Fig. 4 illustrates qualitatively how the curvature of electrodes in toroidal ion traps results in this shift when the AR of the trap is changed. This figure also shows how the broader inner electrode and the narrower outer electrode, as seen in the r-z plane of the asymmetric TorIT (Fig. 4(a)),

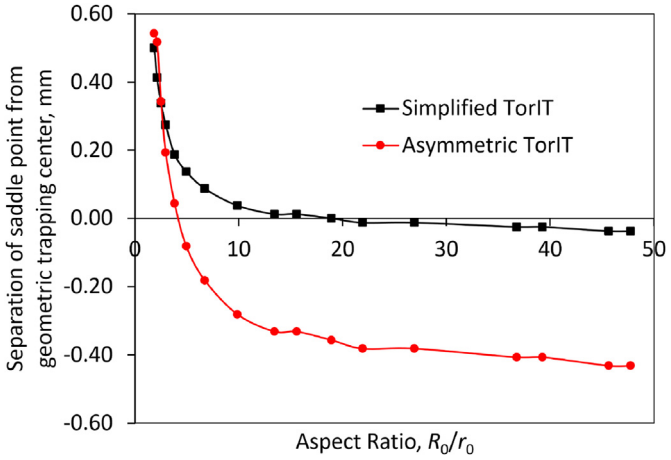

Fig. 3. Separation between the saddle point of the trapping potential and the geometric trap center in the asymmetric TorIT and simplified TorIT as a function of the aspect ratio. The displacement is along the radial direction, r, in both types of traps. Positive values indicate that the saddle point is closer to the rotational axis, or center of the device.

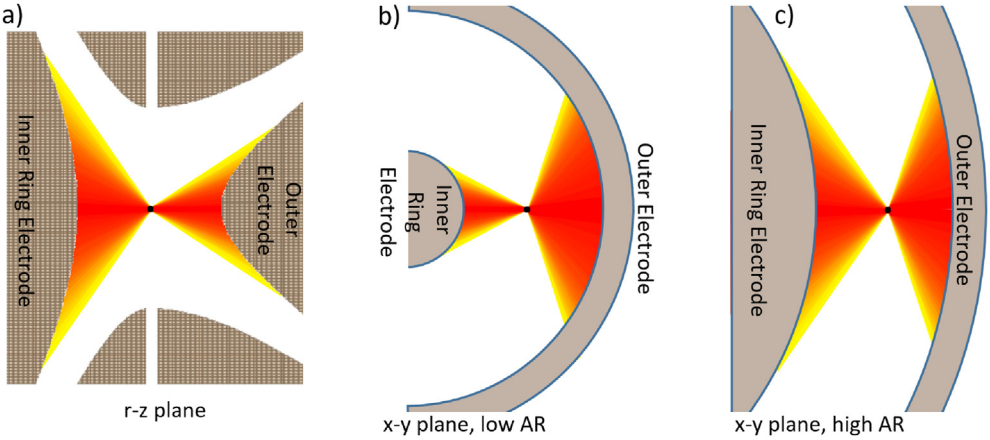

Fig. 4. Qualitative illustration of (a) r-z view and (b) x-y of the Asymmetric TorIT with a test charge at the trapping center. The magnitude of the Coulombic force on the test charge from each point on the electrode surface depends on distance to the surface, which is illustrated with the shaded lines. The asymmetry in the widths of inner and outer electrodes seen in the r-z view cancels the curvature of inner and outer electrodes seen in the x-y view. In (c), an x-y view of a trap with higher aspect ratio, these effects cancel at a different point, and the trapping center shifts.

compensates for the curvature of the electrodes seen in the x-y (r) plane. These factors never exactly cancel except by coincidence or if intentionally so designed; hence the trapping center and geometric center do not generally coincide. When the AR is small, the shape of the trapping potential is most sensitive to small changes in curvature of the electrodes, with this sensitivity dropping off at higher values of AR, as seen in Fig. 3. In the limit of very large AR, the saddle point and geometric center asymptotically approach constant, non-zero values, as expected due to the asymmetry in the electrode cross section.

Fig. 5 shows how the ion secular frequencies vary with AR for both types of traps, while keeping the electrode cross-section constant. The change in curvature causes the secular frequencies to vary in the same way as it changes the higher-order terms in the trapping potential. Similar to the trends in Figs. 2–3, Fig. 5 shows that the behavior of a toroidal trap varies significantly but smoothly for AR changes below approximately AR = 10, and varies much less when the AR is above this value. At AR values higher than this, electrode curvature has less of an effect on ion behavior. These observations agree with predictions using Kotana and Mohanty's approach [22] for calculating secular frequencies using numerical methods.

Within each trap design, and for all values of AR, the radial and axial secular frequencies are nearly degenerate. This is similar to what is observed in a linear ion trap, but quite different from the behavior of a 3-dimensional (3-D) quadrupole ion trap. In the latter case, the r- and z-secular frequencies typically differ by a factor of the square root of 2. This demonstrates that a toroidal trap is more correctly thought of as a linear or 2-dimensional trap with added curvature than as a type of 3-D trap, even for toroidal traps at the limit of low AR.

Fig. 5 also shows that ions do not have stable trajectories in the asymmetric toroidal ion trap at infinite AR (essentially a linear ion trap with the same cross section as the asymmetric toroidal trap). Apparently this AR is too far away from the AR for which this trap was originally designed and optimized, and the deviation in the trapping potential is too great to trap ions. In contrast, the simplified TorIT was originally designed and optimized for a higher AR, so the infinite AR case represents a smaller deviation from the original design.

Ion ejection efficiencies using dipolar resonance ejection in the simplified TorIT were investigated, as shown in Fig. 6. Due to higher-order terms in the trapping potential, the AC frequency corresponding to maximum ejection efficiency was slightly off from

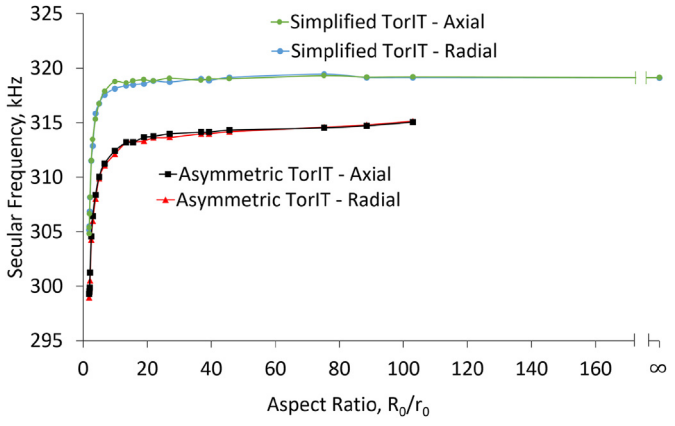

Fig. 5. Effect of aspect ratio on the secular frequency of simplified (r_0 = 5.8 mm) and asymmetric (r_0 = 10.0 mm) TorITs for an ion of m/z = 100. The conditions applied to the trap were 500 $V_{0\text{-}p}$ RF voltage at 1 MHz with no DC offset and no collision gas. The last point for the simplified TorIT represents the secular frequencies of a linear trap with the corresponding (asymmetric) electrode geometry. Ions were not stable in the Asymmetric TorIT with AR above 105.

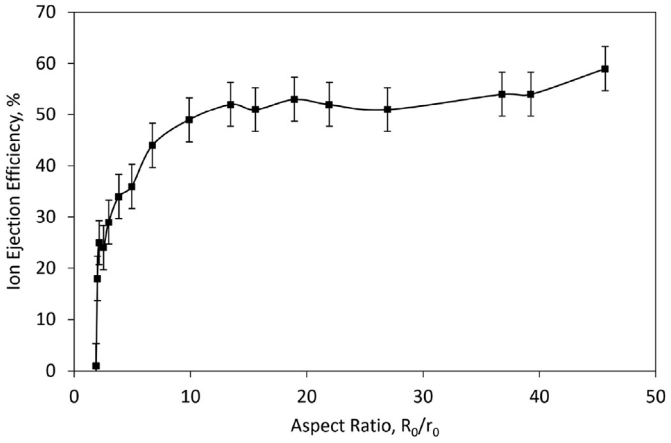

Fig. 6. Ion ejection efficiency of simplified TorIT (ejection in the radial direction). AC voltage applied on the endcap electrode ($V_{0\text{-}p}$ = 2 V) to excite the ion with m/z of 100 via dipolar resonant ejection. The hard sphere collision cooling technique was incorporated under the pressure and temperature of 1.5 mTorr and 273 K respectively.

the ions' secular frequencies before excitation. The frequency for the AC waveform in this simulation was set to a value that is a few percent lower than the exact secular frequency of the ion in the absence of excitation. This auxiliary AC frequency was determined empirically and represents the frequency with maximum ion ejection. During ejection, some ions impacted the wall of the slit or the outer ring electrode of the trap, and other ions were not sufficiently excited to be ejected. A small positive DC voltage on outer ring electrode and small negative DC voltage on inner electrode reduced the outward ion ejection.

As seen in Fig. 6, the ion ejection efficiency follows the same general trend as all of the higher-order terms and the secular frequency: specifically, each parameter shows sharp change with AR at low values of AR, and approaches a constant value for larger AR values, with the transition in behavior occurring around AR = 10. This is not surprising, given that ion ejection from traps has some dependence on non-linear effects. In addition, the dependency of secular frequency on AR has some contribution on the ion ejection efficiency as ions do not eject at the same beta value at different ARs. This effect is very dominant at lower ARs and has less of an effect after the secular frequency flattens off with larger AR.

4. Conclusion

The aspect ratio (AR) of an ion trap directly affects the trapping capacity and sensitivity of the resulting mass spectrometer and represents an important variable in miniaturization efforts. A unique consequence of varying the AR in toroidal traps is the resulting change in the shape of the trapping potential. "Curvature effects" can be understood in terms of higher-order terms of the potential, and affect secular frequencies, ion ejection, and the location of the trapping center. Traps with smaller AR are more sensitive to these curvature effects, and for a given AR, the electrode design must be optimized for performance. These studies show that curvature effects change very little about AR of ~10. The secular frequencies of ions show that toroidal ion traps more closely resemble linear ions traps with added curvature, rather than 3-D quadrupole ion traps, and indeed, a toroidal ion trap with infinite AR is just a linear ion trap with an asymmetric cross section. Finally, the dependency of the secular frequency on AR could help determine other important parameters such as the beta value of the ions, and may lead to improvements in ion ejection efficiency and mass resolution.

Author Statement

Praneeth M. Hettikankanange: Methodology, Software, Validation, Formal analysis, Investigation, Writing – Original Draft; Daniel E. Austin: Writing - Review and Editing, Funding Acquisition, Project Administration, Supervision, Resources, Validation, Conceptualization.

Declaration of competing interest

The authors declare the following financial interests/personal relationships which may be considered as potential competing interests:

The authors report financial support was provided by the U.S. National Science Foundation.

Acknowledgment

The authors gratefully acknowledge funding for this work from the U.S. National Science Foundation (award 2003667) and by the College of Physical and Mathematical Sciences at Brigham Young University.

References

[1] D.E. Austin, M. Wang, S.E. Tolley, J.D. Maas, A.R. Hawkins, A.L. Rockwood, H.D. Tolley, E.D. Lee, M.L. Lee, Halo ion trap mass spectrometer, Anal. Chem. 79 (7) (2007) 2927–2932.
[2] E.R. Badman, R.G. Cooks, A parallel miniature cylindrical ion trap array, Anal. Chem. 72 (14) (2000) 3291–3297.
[3] J.A. Contreras, J.A. Murray, S.E. Tolley, J.L. Oliphant, H.D. Tolley, S.A. Lammert, E.D. Lee, D.W. Later, M.L. Lee, Hand-portable gas chromatograph-toroidal ion trap mass spectrometer (GC-TMS) for detection of hazardous compounds, J. Am. Soc. Mass Spectrom. 19 (10) (2008) 1425–1434.
[4] S.A. Lammert, A.A. Rockwood, M. Wang, M.L. Lee, E.D. Lee, S.E. Tolley, J.R. Oliphant, J.L. Jones, R.W. Waite, Miniature toroidal radio frequency ion trap mass analyzer, J. Am. Soc. Mass Spectrom. 17 (7) (2006) 916–922.
[5] G.E. Patterson, A.J. Guymon, L.S. Riter, M. Everly, J. Griep-Raming, B.C. Laughlin, Z. Ouyang, R.G. Cooks, Miniature cylindrical ion trap mass spectrometer, Anal. Chem. 74 (24) (2002) 6145–6153.
[6] N. Taylor, D.E. Austin, A simplified toroidal ion trap mass analyzer, Int. J. Mass Spectrom. 321–322 (2012) 25–32.
[7] Q. Wu, A. Li, Y. Tian, R.N. Zare, D.E. Austin, Miniaturized linear wire ion trap mass analyzer, Anal. Chem. 88 (15) (2016) 7800–7806.
[8] Z. Ouyang, G. Wu, Y. Song, H. Li, W.R. Plass, R.G. Cooks, Rectilinear ion trap: concepts, calculations, and analytical performance of a new mass analyzer, Anal. Chem. 76 (16) (2004) 4595–4605.
[9] R.W. Gamage, D.E. Austin, The effects of electrode misalignments on the performance of a miniaturized linear wire ion trap mass spectrometer, Int. J. Mass Spectrom. 453 (2020) 116344.
[10] W. Xu, W.J. Chappell, R.G. Cooks, Z. Ouyang, Characterization of electrode surface roughness and its impact on ion trap mass analysis, J. Mass Spectrom. 44 (3) (2009) 353–360.
[11] Y. Peng, B.J. Hansen, H. Quist, Z. Zhang, M. Wang, A.R. Hawkins, D.E. Austin, Coaxial ion trap mass spectrometer: concentric toroidal and quadrupolar trapping regions, Anal. Chem. 83 (14) (2011) 5578–5584.
[12] S.A. Lammert, W.R. Plass, C.V. Thompson, M.B. Wise, Design, optimization and initial performance of a toroidal RF ion trap mass spectrometer, Int. J. Mass Spectrom. 212 (1–3) (2001) 25–40.
[13] X. Li, R.M. Danell, V.T. Pinnick, A. Grubisic, F. van Amerom, R.D. Arevalo, S.A. Getty, W.B. Brinckerhoff, A.E. Southard, Z.D. Gonnsen, T. Adachi, Mars Organic Molecule Analyzer (MOMA) laser desorption/ionization source design and performance characterization, Int. J. Mass Spectrom. 422 (2017) 177–187.
[14] Y. Wang, X. Zhang, Y. Feng, R. Shao, X. Xiong, X. Fang, Y. Deng, W. Xu, Characterization of geometry deviation effects on ion trap mass analysis: a comparison study, Int. *J. Mass Spectrom*. 370 (2014) 125–131.
[15] J.M. Higgs, D.E. Austin, Simulations of ion motion in toroidal ion traps, Int. J. Mass Spectrom. 363 (2014) 40–51.
[16] Z.P. Zhang, H. Quist, Y. Peng, B.J. Hansen, J. Wang, A.R. Hawkins, D.E. Austin, Effects of higher-order multipoles on the performance of a two-plate quadrupole ion trap mass analyzer, Int. J. Mass Spectrom. 299 (2011) 151–157.
[17] Y. Tian, J. Higgs, A. Li, B. Barney, D.E. Austin, How far can ion trap miniaturization go? Parameter scaling and space-charge limits for very small cylindrical ion traps: ion trap miniaturization, J. Mass Spectrom. 49 (3) (2014) 233–240.
[18] A. Chaudhary, F.H.W. van Amerom, R.T. Short, Fabrication and testing of a miniature cylindrical ion trap mass spectrometer constructed from low temperature co-fired ceramics, Int. J. Mass Spectrom. 251 (2006) 32–39.
[19] D.E. Austin, B.J. Hansen, Y. Peng, Z.P. Zhang, Multipole expansion in quadrupolar devices comprised of planar electrode arrays, Int. J. Mass Spectrom. 295 (2010) 153–158.
[20] R.E. March, J.F.J. Todd (Eds.), Practical Aspects of Ion Trap Mass Spectrometry, ume I, CRC Press, Boca Raton, FL, 1995.
[21] E.C. Beaty, Calculated electrostatic properties of ion traps, Phys. Rev. A Gen. Phys. 33 (6) (1986) 3645–3656.
[22] A.N. Kotana, A.K. Mohanty, Determination of multipole coefficients in toroidal ion trap mass analysers, Int. J. Mass Spectrom. 408 (2016) 62–76.